Table 5. Predicted upstream regulators belonging to transcription factors after ONC.

Name	Predicted activation	Activation Z-score	*P*-value of overlap	Target molecules in dataset
ATF4	Activated	3.12	8.90E-18	AARS, ASNS, ATF3, CDKN1A, DDIT3, GARS, LGALS3, MTHFD2, PSAT1, SARS, SERPINF1, SHMT2, SLC7A3, SLC7A5, TNFRSF12A, TRIB3
TP53	Activated	2.44	2.83E-05	ATF3, ATG10, C1QC, CDKN1A, CLIC4, DUSP1, HMGN2, HMOX1, IFI30, IGFBP3, KRT18, LGALS3, MMP9, SERPINB9, SESN2, TMEM43, TRIB3
NFE2L2	Activated	2.13	4.79E-03	ADCYAP1, ARHGEF3, CELA1, FXYD1, HAX1, HMOX1, PSAT1, SRXN1
DDIT3	Activated	2.00	3.20E-06	ATF3, ITGAM, SARS, TRIB3

Data were analyzed with Fisher's exact test. Differences were considered significant with a $P<0.05$ and $|Z\text{-score}| \geq 2$.
doi:10.1371/journal.pone.0093258.t005

that was repeated in our study. The immune system might also play an important role in the pathogenesis of axonal injury.

Conclusion

We used RNA-seq technology to investigate the entire retinal transcriptome profile in the early stages of post-axonal injury. A pathway analysis of DEGs indicated that cell death and the survival response were induced at an early stage after ONC. ER

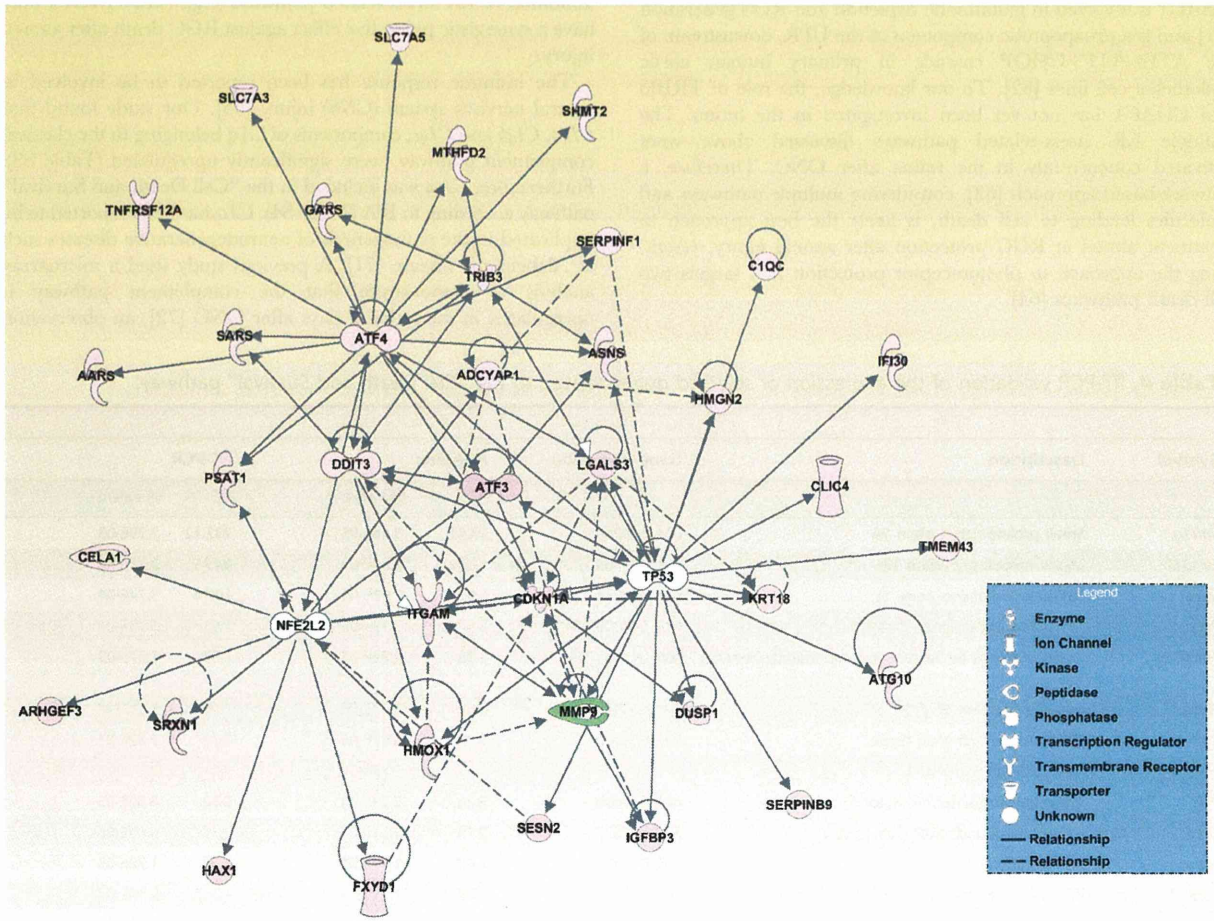

Figure 3. Interaction networks involved in axonal injury after ONC. The upstream analysis was performed with IPA. ATF4, TP53, NFE2L2, DDIT3 and the target molecules of these upstream regulators were merged for this representation of the interaction networks after ONC.
doi:10.1371/journal.pone.0093258.g003

stress was the main response in axonal injury, inducing many other pathways (i.e., RGC marker down regulation, the antioxidative response, the immune response, and axon regeneration). Our transcriptomic approach to this investigation, which relied on RNA-seq, was a powerful and effective method, and allowed us to obtain a global view of gene expression changes in the retina after axonal injury. We believe that our study has provided new insights into the molecular mechanisms underlying axonal damage, and may help in research aimed at the discovery of new biomarkers and therapeutic targets for a variety of ocular diseases.

Materials and Methods

Animals

C57BL/6 mice (male, 12-week-old; SLC, Hamamatsu, Japan) were used in this study. The surgical procedures were performed under deep anesthesia with intramuscular administration of a mixture of ketamine (100 mg/kg) and xylazine (9 mg/kg). All animals were maintained and handled in accordance with the guidelines of the ARVO Statement for the Use of Animals in Ophthalmic and Vision Research and the guidelines from the declaration of Helsinki and the Guiding Principles in the Care and Use of Animals. All experimental procedures described in the present study were approved by the Ethics Committee for Animal Experiments at Tohoku University Graduate School of Medicine, and were performed according to the National Institutes of Health guidelines for the care and use of laboratory animals.

Induction of axonal injury in mice

ONC was used to induce axonal injury as previously described [10]. Briefly, the optic nerve was exposed, crushed 2 mm posterior to the globe with fine forceps for 10 seconds, and released. A fundus examination was used to confirm the appearance of normal blood circulation, and antibiotic ointment was applied. The operation was similar in the sham group, but after exposure, the optic nerve was not crushed.

RNA extraction

Two days after surgery, the retinas of the mice were extracted and immediately immersed in an RNA stabilization reagent (RNase later sample and assay technology; Qiagen, Valencia, CA). The retinas were then homogenized in Qiazol (Qiagen) with a pestle homogenizer, and total RNA was extracted from the homogenized mixture with a miRNeasy mini kit (Qiagen). The resulting 48 individual samples (24 from the ONC group and 24 from the control group) were then assessed with a spectrophotometer to determine their total RNA concentration (NanoDrop 2000c, Thermo Scientific).

RNA sequencing

Thirty-six samples of purified RNA (18 from the ONC and 18 from the control group) were used for this analysis. In each group, fixed quantities of RNA were taken from six samples and combined into a single sample, in order to minimize the influence of individual variations in the mice. This process yielded three combined samples from both the ONC and control groups. The quality of these six combined RNA samples was then assessed with an Agilent 2100 Bioanalyzer (Agilent Technologies, Palo Alto, CA). The triplicated ONC and control samples used for the RNA-seq analysis had RNA integrity numbers (RIN) ranging from 7.8 to 8.2 (Table S1). The cDNA library of each sample was prepared with Illumina Tru-Seq RNA Sample Prep Kits (Illumina, San Diego, CA) for 100 bp paired-end reads, according to the manufacturer's instructions. Each of the six cDNA libraries was indexed for multiplexing. These six indexed libraries were sequenced on one lane of the Illumina Hiseq2000 device.

Data were recorded in the FASTQ format and then imported to CLC Genomics Workbench (version 6.0.1) (CLC Bio, Aarhus, Denmark) for analysis [18,19]. All sequence reads were mapped to the reference genome (NCBI37/mm9) with the RNA-seq mapping algorithm included in CLC Genomics Workbench. The maximum number of mismatches allowed for the mapping was set at 2. To estimate gene expression levels, we calculated RPKM with CLC Genomics Workbench, as defined by Mortazavi et al. [20], and then analyzed differentially expressed genes (DEGs) in the control and ONC samples. All sequence data have been deposited in the Gene Expression Omnibus under the accession number GSE55228.

Quantitative RT-PCR

Twelve samples of purified RNA (6 from the ONC and 6 from the control group) were used for quantitative RT-PCR. Total RNA (200 ng per sample) from the samples was first reverse-transcribed into cDNA using SuperScript III (Invitrogen Life Technologies, Carlsbad, CA). Quantitative RT-PCR was then performed with a 7500 Fast Real-Time PCR System (Applied Biosystems, Foster City, CA) as previously described, with minor modifications [73]. For each 20 µl reaction the following were used: 10 µl TaqMan Fast Universal PCR Master Mix (Applied Biosystems, Foster City, CA), 1 µl Taqman probe, 1 µl template DNA, and 8 µl DEPC water. Each sample was run in duplicate in each assay. For a relative comparison of gene expression, we analyzed the results of the real-time PCR data with the comparative Ct method ($2^{-\Delta\Delta CT}$), normalized to *Gapdh*, an endogenous control. All Taqman probes used for these reactions are listed in Table S5.

Pathway analysis

Pathway and global functional analyses were performed with IPA software [36,74,75]. The DEG datasets were uploaded to the IPA application and mapped to IPKB. Each gene identifier was then mapped to its corresponding IPKB. Networks of these genes were generated based on their connectivity. The significance of the association between the datasets and biofunctions were measured using a ratio of number of genes from the dataset that map to the pathway divided by the total number of genes in that pathway. An upstream regulator analysis was performed to compare DEGs in the datasets to those known to be regulated by a given upstream regulator. Based on the concordance between them, an activation score was assigned, showing whether a potential transcriptional regulator was in an "activated" (z score ≥ 2), "inhibited" (z score ≤ -2), or uncertain state.

Statistical analysis

RNA-seq data were analyzed and RPKM was calculated with CLC Genomics Workbench [76]. A threshold RPKM value of 0.3 has been reported to balance the numbers of false positives and false negatives [21,77]. We therefore excluded genes that did not have RPKM > 0.3 in at least one group. This yielded 13160 genes, which we then used in the differential expression analysis. *P*-values were calculated with the Student's t-test and were adjusted for multiplicity with the Bioconductor package qvalue [78,79]. This software allows for selecting statistically significant genes while controlling the estimated false discovery rate (FDR). FDR < 0.1 with $|FC| > 1.5$ was considered statistically significant in the RNA-seq analysis. RT-PCR data were analyzed with the Welch's t-test. Statistical analysis of the RNA-seq and RT-PCR data was performed with R software (version 3.0.1) [22].

The significance of the pathway analysis was calculated with Fisher's exact test in the IPA application. If the *P*-values for RT-PCR and IPA were less than 0.05, the result was considered statistically significant.

Supporting Information

Table S1 RNA integrity numbers and summary of sequence statistics.
(XLSX)

Table S2 Detailed mapping statistics.
(XLSX)

Table S3 List of DEGs after ONC.
(XLSX)

Table S4 List of DEGs belonging to cell death and survival after ONC.
(XLSX)

Table S5 List of Taqman probes used in this study.
(DOCX)

Acknowledgments

We thank Ms. Junko Sato and Ms. Dilinuer Maimaitishawuti for technical assistance.

Author Contributions

Conceived and designed the experiments: MY TN YT MR. Performed the experiments: MY YT ST. Analyzed the data: MY YT. Contributed reagents/materials/analysis tools: MY YT. Wrote the paper: MY.

References

1. Kwon YH, Fingert JH, Kuehn MH, Alward WL (2009) Primary open-angle glaucoma. New England Journal of Medicine 360: 1113–1124.
2. Weinreb RN, Khaw PT (2004) Primary open-angle glaucoma. The Lancet 363: 1711–1720.
3. Calkins DJ (2012) Critical pathogenic events underlying progression of neurodegeneration in glaucoma. Prog Retin Eye Res 31: 702–719.
4. Heijl A, Leske MC, Bengtsson B, Hyman L, Bengtsson B, et al. (2002) Reduction of intraocular pressure and glaucoma progression: results from the Early Manifest Glaucoma Trial. Arch Ophthalmol 120: 1268–1279.
5. Collaborative Normal-Tension Glaucoma Study Group (1998) The effectiveness of intraocular pressure reduction in the treatment of normal-tension glaucoma. Am J Ophthalmol 126: 498–505.
6. Hollands H, Johnson D, Hollands S, Simel DL, Jinapriya D, et al. (2013) Do findings on routine examination identify patients at risk for primary open-angle glaucoma? The rational clinical examination systematic review. JAMA : the journal of the American Medical Association 309: 2035–2042.
7. De Moraes CGV, Juthani VJ, Liebmann JM, Teng CC, Tello C, et al. (2011) Risk factors for visual field progression in treated glaucoma. Archives of ophthalmology 129: 562–568.
8. Nakazawa T, Chiba N, Omodaka K, Yokoyama Y, Aizawa N, et al. (2011) Association between optic nerve blood flow and objective examinations in glaucoma patients with generalized enlargement disc type. Clinical ophthalmology (Auckland, NZ): 1549.
9. Himori N, Yamamoto K, Maruyama K, Ryu M, Taguchi K, et al. (2013) Critical role of Nrf2 in oxidative stress-induced retinal ganglion cell death. J Neurochem.
10. Ryu M, Yasuda M, Shi D, Shanab AY, Watanabe R, et al. (2012) Critical role of calpain in axonal damage-induced retinal ganglion cell death. J Neurosci Res 90: 802–815.
11. Fujimoto JG (2003) Optical coherence tomography for ultrahigh resolution in vivo imaging. Nat Biotechnol 21: 1361–1367.
12. Allcutt D, Berry M, Sievers J (1984) A qualitative comparison of the reactions of retinal ganglion cell axons to optic nerve crush in neonatal and adult mice. Brain Res 318: 231–240.
13. Li Y, Schlamp CL, Nickells RW (1999) Experimental induction of retinal ganglion cell death in adult mice. Invest Ophthalmol Vis Sci 40: 1004–1008.
14. Libby RT, Li Y, Savinova OV, Barter J, Smith RS, et al. (2005) Susceptibility to neurodegeneration in a glaucoma is modified by Bax gene dosage. PLoS Genet 1: 17–26.
15. Weinreb RN, Friedman DS, Fechtner RD, Cioffi GA, Coleman AL, et al. (2004) Risk assessment in the management of patients with ocular hypertension. Am J Ophthalmol 138: 458–467.
16. Fischer D, Petkova V, Thanos S, Benowitz LI (2004) Switching mature retinal ganglion cells to a robust growth state in vivo: gene expression and synergy with RhoA inactivation. The Journal of neuroscience : the official journal of the Society for Neuroscience 24: 8726–8740.
17. Wang Z, Gerstein M, Snyder M (2009) RNA-Seq: a revolutionary tool for transcriptomics. Nature reviews Genetics 10: 57–63.
18. Tong M, Chan KW, Bao JY, Wong KY, Chen JN, et al. (2012) Rab25 is a tumor suppressor gene with antiangiogenic and anti-invasive activities in esophageal squamous cell carcinoma. Cancer Res 72: 6024–6035.
19. Greenwald JW, Greenwald CJ, Philmus BJ, Begley TP, Gross DC (2012) RNA-seq analysis reveals that an ECF sigma factor, AcsS, regulates achromobactin biosynthesis in Pseudomonas syringae pv. syringae B728a. PLoS One 7: e34804.
20. Mortazavi A, Williams BA, McCue K, Schaeffer L, Wold B (2008) Mapping and quantifying mammalian transcriptomes by RNA-Seq. Nat Methods 5: 621–628.
21. Ramskold D, Wang ET, Burge CB, Sandberg R (2009) An abundance of ubiquitously expressed genes revealed by tissue transcriptome sequence data. PLoS Comput Biol 5: e1000598.
22. Team RC (2013) R: A Language and Environment for Statistical Computing. R Foundation for Statistical Computing, Vienna, Austria. Available: http://www.R-project.org.
23. Storey JD, Tibshirani R (2003) Statistical significance for genomewide studies. Proc Natl Acad Sci U S A 100: 9440–9445.
24. Huang TH, Uthe JJ, Bearson SM, Demirkale CY, Nettleton D, et al. (2011) Distinct peripheral blood RNA responses to Salmonella in pigs differing in Salmonella shedding levels: intersection of IFNG, TLR and miRNA pathways. PLoS One 6: e28768.
25. Kamei S, Chen-Kuo-Chang M, Cazevieille C, Lenaers G, Olichon A, et al. (2005) Expression of the Opa1 mitochondrial protein in retinal ganglion cells: its downregulation causes aggregation of the mitochondrial network. Invest Ophthalmol Vis Sci 46: 4288–4294.
26. Fernandes KA, Harder JM, Kim J, Libby RT (2013) JUN regulates early transcriptional responses to axonal injury in retinal ganglion cells. Exp Eye Res 112: 106–117.
27. Wickham H (2009) ggplot2: elegant graphics for data analysis. Springer New York.
28. Ward Jr JH (1963) Hierarchical grouping to optimize an objective function. Journal of the American statistical association 58: 236–244.
29. Warnes GR, Bolker B, Bonebakker L, Gentleman R, Huber W, et al. (2013) gplots: Various R programming tools for plotting data. R package version 2.12.1. http://CRAN.R-project.org/package = gplots.
30. Nadal-Nicolas FM, Jimenez-Lopez M, Sobrado-Calvo P, Nieto-Lopez L, Canovas-Martinez I, et al. (2009) Brn3a as a marker of retinal ganglion cells: qualitative and quantitative time course studies in naive and optic nerve-injured retinas. Invest Ophthalmol Vis Sci 50: 3860–3868.
31. Kim CY, Kuehn MH, Clark AF, Kwon YH (2006) Gene expression profile of the adult human retinal ganglion cell layer. Mol Vis 12: 1640–1648.
32. Chidlow G, Casson R, Sobrado-Calvo P, Vidal-Sanz M, Osborne NN (2005) Measurement of retinal injury in the rat after optic nerve transection: an RT-PCR study. Mol Vis 11: 387–396.
33. Liang SH, Zhang W, McGrath BC, Zhang P, Cavener DR (2006) PERK (eIF2alpha kinase) is required to activate the stress-activated MAPKs and induce the expression of immediate-early genes upon disruption of ER calcium homoeostasis. Biochem J 393: 201–209.
34. Ohoka N, Yoshii S, Hattori T, Onozaki K, Hayashi H (2005) TRB3, a novel ER stress-inducible gene, is induced via ATF4-CHOP pathway and is involved in cell death. EMBO J 24: 1243–1255.
35. Logue SE, Cleary P, Saveljeva S, Samali A (2013) New directions in ER stress-induced cell death. Apoptosis 18: 537–546.
36. Ramayo-Caldas Y, Mach N, Esteve-Codina A, Corominas J, Castello A, et al. (2012) Liver transcriptome profile in pigs with extreme phenotypes of intramuscular fatty acid composition. BMC Genomics 13: 547.
37. Levkovitch-Verbin H, Harris-Cerruti C, Groner Y, Wheeler LA, Schwartz M, et al. (2000) RGC death in mice after optic nerve crush injury: oxidative stress and neuroprotection. Invest Ophthalmol Vis Sci 41: 4169–4174.
38. Villegas-Perez MP, Vidal-Sanz M, Rasminsky M, Bray GM, Aguayo AJ (1993) Rapid and protracted phases of retinal ganglion cell loss follow axotomy in the optic nerve of adult rats. J Neurobiol 24: 23–36.
39. Berkelaar M, Clarke DB, Wang YC, Bray GM, Aguayo AJ (1994) Axotomy results in delayed death and apoptosis of retinal ganglion cells in adult rats. J Neurosci 14: 4368–4374.
40. Nakazawa T, Takahashi H, Nishijima K, Shimura M, Fuse N, et al. (2007) Pitavastatin prevents NMDA-induced retinal ganglion cell death by suppressing leukocyte recruitment. J Neurochem 100: 1018–1031.
41. Lam TT, Abler AS, Kwong JM, Tso MO (1999) N-methyl-D-aspartate (NMDA)–induced apoptosis in rat retina. Invest Ophthalmol Vis Sci 40: 2391–2397.

42. Siliprandi R, Canella R, Carmignoto G, Schiavo N, Zanellato A, et al. (1992) N-methyl-D-aspartate-induced neurotoxicity in the adult rat retina. Vis Neurosci 8: 567–573.
43. Seki T, Nakatani M, Taki C, Shinohara Y, Ozawa M, et al. (2006) Neuroprotective effect of PACAP against kainic acid-induced neurotoxicity in rat retina. Ann N Y Acad Sci 1070: 531–534.
44. Ehrlich D, Teuchert G, Morgan IG (1987) Specific ganglion cell death induced by intravitreal kainic acid in the chicken retina. Brain Res 415: 342–346.
45. Honjo M, Tanihara H, Kido N, Inatani M, Okazaki K, et al. (2000) Expression of ciliary neurotrophic factor activated by retinal Muller cells in eyes with NMDA- and kainic acid-induced neuronal death. Invest Ophthalmol Vis Sci 41: 552–560.
46. Nakazawa T, Nakazawa C, Matsubara A, Noda K, Hisatomi T, et al. (2006) Tumor necrosis factor-alpha mediates oligodendrocyte death and delayed retinal ganglion cell loss in a mouse model of glaucoma. J Neurosci 26: 12633–12641.
47. Kitaoka Y, Kitaoka Y, Kwong JM, Ross-Cisneros FN, Wang J, et al. (2006) TNF-alpha-induced optic nerve degeneration and nuclear factor-kappaB p65. Invest Ophthalmol Vis Sci 47: 1448–1457.
48. Liu Y, Tang L, Chen B (2012) Effects of antioxidant gene therapy on retinal neurons and oxidative stress in a model of retinal ischemia/reperfusion. Free Radic Biol Med 52: 909–915.
49. Nakazawa T, Shimura M, Ryu M, Nishida K, Pages G, et al. (2008) ERK1 plays a critical protective role against N-methyl-D-aspartate-induced retinal injury. J Neurosci Res 86: 136–144.
50. Watkins TA, Wang B, Huntwork-Rodriguez S, Yang J, Jiang Z, et al. (2013) DLK initiates a transcriptional program that couples apoptotic and regenerative responses to axonal injury. Proceedings of the National Academy of Sciences of the United States of America 110: 4039–4044.
51. Almasieh M, Wilson AM, Morquette B, Cueva Vargas JL, Di Polo A (2012) The molecular basis of retinal ganglion cell death in glaucoma. Prog Retin Eye Res 31: 152–181.
52. Chidlow G, Casson R, Sobrado-Calvo P, Vidal-Sanz M, Osborne NN (2005) Measurement of retinal injury in the rat after optic nerve transection: an RT-PCR study. Molecular vision 11: 387–396.
53. Quina LA, Pak W, Lanier J, Banwait P, Gratwick K, et al. (2005) Brn3a-expressing retinal ganglion cells project specifically to thalamocortical and collicular visual pathways. J Neurosci 25: 11595–11604.
54. Soto I, Oglesby E, Buckingham BP, Son JL, Roberson EDO, et al. (2008) Retinal ganglion cells downregulate gene expression and lose their Axons within the optic nerve head in a mouse glaucoma model. Journal of Neuroscience 28: 548–561.
55. Leon S, Yin Y, Nguyen J, Irwin N, Benowitz LI (2000) Lens injury stimulates axon regeneration in the mature rat optic nerve. J Neurosci 20: 4615–4626.
56. Roussel BD, Kruppa AJ, Miranda E, Crowther DC, Lomas DA, et al. (2013) Endoplasmic reticulum dysfunction in neurological disease. Lancet Neurol 12: 105–118.
57. Kim I, Xu W, Reed JC (2008) Cell death and endoplasmic reticulum stress: disease relevance and therapeutic opportunities. Nat Rev Drug Discov 7: 1013–1030.
58. Oyadomari S, Mori M (2004) Roles of CHOP/GADD153 in endoplasmic reticulum stress. Cell Death Differ 11: 381–389.
59. Hu Y, Park KK, Yang L, Wei X, Yang Q, et al. (2012) Differential effects of unfolded protein response pathways on axon injury-induced death of retinal ganglion cells. Neuron 73: 445–452.
60. Urano F, Wang X, Bertolotti A, Zhang Y, Chung P, et al. (2000) Coupling of stress in the ER to activation of JNK protein kinases by transmembrane protein kinase IRE1. Science 287: 664–666.
61. Kumar A, Tikoo S, Maity S, Sengupta S, Sengupta S, et al. (2012) Mammalian proapoptotic factor ChaC1 and its homologues function as gamma-glutamyl cyclotransferases acting specifically on glutathione. EMBO Rep 13: 1095–1101.
62. Mungrue IN, Pagnon J, Kohannim O, Gargalovic PS, Lusis AJ (2009) CHAC1/MGC4504 is a novel proapoptotic component of the unfolded protein response, downstream of the ATF4-ATF3-CHOP cascade. J Immunol 182: 466–476.
63. Barabasi AL, Gulbahce N, Loscalzo J (2011) Network medicine: a network-based approach to human disease. Nat Rev Genet 12: 56–68.
64. Trichonas G, Murakami Y, Thanos A, Morizane Y, Kayama M, et al. (2010) Receptor interacting protein kinases mediate retinal detachment-induced photoreceptor necrosis and compensate for inhibition of apoptosis. Proc Natl Acad Sci U S A 107: 21695–21700.
65. Barnham KJ, Masters CL, Bush AI (2004) Neurodegenerative diseases and oxidative stress. Nat Rev Drug Discov 3: 205–214.
66. Harada C, Namekata K, Guo X, Yoshida H, Mitamura Y, et al. (2010) ASK1 deficiency attenuates neural cell death in GLAST-deficient mice, a model of normal tension glaucoma. Cell death and differentiation 17: 1751–1759.
67. Kensler TW, Wakabayashi N, Biswal S (2007) Cell survival responses to environmental stresses via the Keap1-Nrf2-ARE pathway. Annu Rev Pharmacol Toxicol 47: 89–116.
68. Singh A, Ling G, Suhasini AN, Zhang P, Yamamoto M, et al. (2009) Nrf2-dependent sulfiredoxin-1 expression protects against cigarette smoke-induced oxidative stress in lungs. Free Radic Biol Med 46: 376–386.
69. Tanaka H, Yamashita T, Yachi K, Fujiwara T, Yoshikawa H, et al. (2004) Cytoplasmic p21(Cip1/WAF1) enhances axonal regeneration and functional recovery after spinal cord injury in rats. Neuroscience 127: 155–164.
70. Chen W, Sun Z, Wang XJ, Jiang T, Huang Z, et al. (2009) Direct interaction between Nrf2 and p21(Cip1/WAF1) upregulates the Nrf2-mediated antioxidant response. Mol Cell 34: 663–673.
71. Crehan H, Holton P, Wray S, Pocock J, Guerreiro R, et al. (2012) Complement receptor 1 (CR1) and Alzheimer's disease. Immunobiology 217: 244–250.
72. Templeton JP, Freeman NE, Nickerson JM, Jablonski MM, Rex TS, et al. (2013) Innate immune network in the retina activated by optic nerve crush. Invest Ophthalmol Vis Sci 54: 2599–2606.
73. Shanab AY, Nakazawa T, Ryu M, Tanaka Y, Himori N, et al. (2012) Metabolic stress response implicated in diabetic retinopathy: The role of calpain, and the therapeutic impact of calpain inhibitor. Neurobiology of disease 48: 556–567.
74. Prat-Vidal C, Gálvez-Montón C, Nonell L, Puigdecanet E, Astier L, et al. (2013) Identification of Temporal and Region-Specific Myocardial Gene Expression Patterns in Response to Infarction in Swine. PLoS ONE 8: e54785.
75. Saili KS, Tilton SC, Waters KM, Tanguay RL (2013) Global gene expression analysis reveals pathway differences between teratogenic and non-teratogenic exposure concentrations of bisphenol A and 17β-estradiol in embryonic zebrafish. Reproductive Toxicology 38: 89–101.
76. Gusberti M, Gessler C, Broggini GA (2013) RNA-Seq Analysis Reveals Candidate Genes for Ontogenic Resistance in Malus-Venturia Pathosystem. PLoS One 8: e78457.
77. Rowley JW, Weyrich AS (2013) Coordinate expression of transcripts and proteins in platelets. Blood 121: 5255–5256.
78. Dabney A, Storey JD qvalue: Q-value estimation for false discovery rate control. R package version 1.36.0.
79. Folkersen L, Kyriakou T, Goel A, Peden J, Malarstig A, et al. (2009) Relationship between CAD risk genotype in the chromosome 9p21 locus and gene expression. Identification of eight new ANRIL splice variants. PLoS One 4: e7677.

The Novel Rho Kinase (ROCK) Inhibitor K-115: A New Candidate Drug for Neuroprotective Treatment in Glaucoma

Kotaro Yamamoto, Kazuichi Maruyama, Noriko Himori, Kazuko Omodaka, Yu Yokoyama, Yukihiro Shiga, Ryu Morin, and Toru Nakazawa

Department of Ophthalmology, Tohoku University Graduate School of Medicine, Sendai, Miyagi, Japan

Correspondence: Toru Nakazawa, Tohoku University Graduate School of Medicine, Department of Ophthalmology, 1-1 Seiryo, Aoba, Sendai, Miyagi, 980-8574, Japan; ntoru@oph.med.tohoku.ac.jp.

Submitted: December 27, 2013
Accepted: September 16, 2014

Citation: Yamamoto K, Maruyama K, Himori N, et al. The novel Rho kinase (ROCK) inhibitor K-115: a new candidate drug for neuroprotective treatment in glaucoma. *Invest Ophthalmol Vis Sci.* 2014;557126-7136. DOI: 10.1167/iovs.13-13842

Purpose. To investigate the effect of K-115, a novel Rho kinase (ROCK) inhibitor, on retinal ganglion cell (RGC) survival in an optic nerve crush (NC) model. Additionally, to determine the details of the mechanism of K-115's neuroprotective effect in vivo and in vitro.

Methods. ROCK inhibitors, including K-115 and fasudil (1 mg/kg/d), or vehicle were administered orally to C57BL/6 mice. Retinal ganglion cell death was then induced with NC. Retinal ganglion cell survival was evaluated by counting surviving retrogradely labeled cells and measuring RGC marker expression with quantitative real-time polymerase chain reaction (qRT-PCR). Total oxidized lipid levels were assessed with a thiobarbituric acid-reactive substances (TBARS) assay. Reactive oxygen species (ROS) levels were assessed by co-labeling with CellROX and Fluorogold. Expression of the NADPH oxidase (Nox) family of genes was evaluated with qRT-PCR.

Results. The survival of RGCs after NC was increased 34 ± 3% with K-115, a significantly protective effect. Moreover, a similar effect was revealed by the qRT-PCR analysis of *Thy-1.2* and *Brn3a*, RGC markers. Levels of oxidized lipids and ROS also increased with time after NC. NC-induced oxidative stress, including oxidation of lipids and production of ROS, was significantly attenuated by K-115. Furthermore, expression of the Nox gene family, especially *Nox1*, which is involved in the NC-induced ROS production pathway, was dramatically reduced by K-115.

Conclusions. The results indicated that oral K-115 administration delayed RGC death. Although K-115 may be mediated through *Nox1* downregulation, we found that it did not suppress ROS production directly. Our findings show that K-115 has a potential use in neuroprotective treatment for glaucoma and other neurodegenerative diseases.

Keywords: oxidative stress, retinal ganglion cell, ROCK, glaucoma, neuroprotection, Nox

Glaucoma is well known as one of the world's major causes of secondary blindness,[1] and in Japan in particular, glaucoma is quickly becoming the most common cause of secondary blindness. Maintenance of low intraocular pressure (IOP) is the classic treatment for glaucoma and is the only therapy that has been shown to be effective in large-scale clinical studies. The primary method of reducing IOP is generally medication, mainly topical eye drops, although filtration surgery is also used. These are the only current treatments for glaucoma. Increased IOP is the most well-known risk factor for the progression of glaucoma, and IOP reduction is usually effective in slowing the progress of the disease. However, the majority of glaucoma patients in Asia are affected by normal tension glaucoma (NTG), and recent epidemiological studies have revealed that IOP reduction alone cannot prevent the progression of visual field loss in these patients.[2,3] In addition to reducing IOP, reduction of damage to retinal ganglion cells (RGCs) caused by IOP-independent risk factors such as mechanical stress on the axons in the lamina cribrosa might be useful for treating NTG.[4] Novel treatment strategies have therefore recently been explored, such as protecting RGCs or increasing retinal or choroidal blood flow. In particular, the neuroprotection of RGCs has drawn attention as a new approach to glaucoma therapy because it is thought that the ultimate cause of vision loss in glaucoma is RGC apoptosis.[5]

Several potential mechanisms of RGC death in glaucoma have been hypothesized, including compromised blood flow in the optic nerve,[6,7] nitric oxide–induced injury to the optic nerve,[8–10] and glutamate excitotoxicity.[11–13] In addition to these primary mechanisms, other studies have provided evidence that oxidative stress contributes to the degeneration of RGCs in glaucoma.[14–17] However, the precise nature of the damage caused to RGCs by oxidative stress remains unclear. Moreover, treatments for oxidative stress in glaucoma patients have not been established.

Rho kinase (ROCK) is a serine/threonine (Ser/Thr) protein kinase and a key downstream effector of Rho.[18,19] ROCK controls multiple signaling pathways and many cellular processes such as cytoskeletal rearrangement and cell movement.[20] Thus, it has recently been suggested that the Rho/ROCK pathway is involved in a number of disorders. Indeed, abnormal activation of ROCK has been observed in diabetic nephropathy,[21–26] cardiovascular disease,[19,24,27–31] and central nervous system (CNS) diseases including Alzheimer's disease,[32–34] spinal cord injury,[32,35–38] stroke,[39–46] multiple sclerosis,[32] and glaucoma.[47–56] In particular, a recent study

www.iovs.org | ISSN: 1552-5783

reported that the protein level of RhoA increased in the optic nerve head of patients with primary open-angle glaucoma (POAG),[57] an effect that might lead to excessive activation of ROCK. Many studies using models such as hypertension, hyperlipidemia, and diabetes have demonstrated that ROCK activation caused elevated oxidative stress levels via NADPH oxidase (Nox), and that this was eliminated by oral administration of the ROCK inhibitor fasudil.[22]

ROCK inhibitors are thought to be one of the most promising candidates for the treatment of glaucoma. Previously, the targeting of small Rho GTPase has been shown to increase regeneration in models of optic nerve lesions.[58] Specifically, pharmacological inhibition of ROCK had a dose-dependent regenerative effect on RGCs after an optic nerve crush (NC) injury.[59] Moreover, selective ROCK inhibitors have also been shown to lower IOP in rabbits,[48] rats,[60] and monkeys.[61] This compound had a direct effect on the trabecular meshwork and the cells in Schlemm's canal. Recent research had provided a great deal of data on the multiple potential therapeutic uses of ROCK inhibitors in glaucoma, including both IOP maintenance[48,53,55,62–65] and RGC neuroprotection.[66]

K-115, an isoquinolinesulfonamide derivative, shows high selectivity for ROCK inhibition, especially ROCK 2. The 50% inhibitory concentration (IC_{50}) of K-115 for ROCK 1, ROCK 2, PKACα, PKC, and CaMKIIα was 0.051, 0.019, 2.1, 27, and 0.37 μM, respectively.[67] In contrast, the IC_{50} of other ROCK inhibitors such as Y-27632 and fasudil was 2 to 18 times higher than that of K-115. This high selectivity contributes to the safety profile of K-115 because different protein kinases have structurally similar active binding sites yet regulate diverse signaling pathways.[32,68] Indeed, phase 1 and 2 clinical trials have indicated that K-115 is a safe topical agent for IOP reduction over an 8-week course of treatment in healthy volunteers and patients with POAG.[69,70]

Methods

Materials

Fluorogold (FG) was purchased from Fluorochrome (Denver, CO, USA). All chemicals used in this study's thiobarbituric acid-reactive substances (TBARS) assays were purchased from Wako Pure Chemicals (Osaka, Japan), except for the protease inhibitor cocktails, which were purchased from Sigma-Aldrich (Tokyo, Japan). K-115, a ROCK inhibitor, was kindly provided free of charge by Kowa Company, Ltd. (Nagoya, Japan). Fasudil was purchased from Tokyo Chemical Industry Co., Ltd. (Tokyo, Japan).

Animals

Nine- to 12-week-old male C57BL/6 mice (SLC, Shizuoka, Japan) were used in this study. The animals in these experiments were used in accordance with the ARVO Statement for the Use of Animals in Ophthalmic and Vision Research and the Guidelines for Animal Experiments of Tohoku University. All animal experiments were conducted with the approval of the Animal Research Committee, Graduate School of Medicine, Tohoku University. Every assay was conducted on a separate set of retinas.

Retrograde Labeling of RGCs and Optic Nerve Surgery

To identify RGCs in the ganglion cell layer (GCL), retrograde labeling was performed 7 days before optic nerve surgery. Labeling was performed by injecting 1 μL of 2% aqueous FG containing 1% dimethylsulfoxide (DMSO) into the superior colliculus, using a Hamilton syringe with a 32-gauge needle. Seven days after retrograde labeling with FG, NC was performed as described previously.[71,72] Briefly, 15 minutes after administration of K-115 or fasudil, the optic nerve was crushed approximately 1 mm posterior to the eyeball without damage to the retinal blood supply. Beginning the day after surgery, K-115 or fasudil (1 mg/kg) was then administered orally once a day for 7 days.

Quantitative Real-Time RT-PCR

The retinas were directly lysed in Qiagen RNeasy RLT Lysis buffer. Subsequent RNA extraction was performed with the RNeasy Micro Kit (Qiagen, Hilden, Germany) according to the manufacturer's instructions. Total RNA (50 ng) was reverse transcribed using a SuperScript III First Strand Synthesis kit (Life Technologies, Inc., MD, USA) to synthesize cDNA. Real-time quantitative RT-PCR was carried out with a 7500 fast real-time PCR system (Applied Biosystems, Foster City, CA, USA) using TaqMan probes (Life Technologies, Inc.). The catalog numbers of the predesigned TaqMan probes were as follows: Thy-1.2 (Mm00493681_m1), Brn3a (Mm02343791_m1), Nox1 (Mm00549170_m1), Nox2 (Mm01287743_m1), Nox3 (Mm01339132_m1), Nox4 (Mm00479246_m1), and GAPDH (Mm99999915_g1). Relative gene expression levels were calculated using the delta-delta Ct method.

TBARS Assay

The TBARS assay was carried out according to previously reported methods[73,74] with minor modifications. TBARS assays measure the total level of oxidized lipids based on the reaction of malondialdehyde (MDA), one of the end products of lipid peroxidation, with thiobarbituric acid (TBA).[75] Briefly, the retinal homogenate, in 1.15% KCl containing 1% protease inhibitor cocktail and 0.5 mM butylated hydroxytoluene (BHT), was added to a reaction mixture (0.81% SDS, 0.36% TBA, and 9% acetic acid) on ice. After heating the reaction mixture to 100°C for 1 hour, it was centrifuged at 20,000*g* for 10 minutes at 4°C. The supernatant was collected and its fluorescence was measured at 530 nm excitation and 550 nm emission. The results were normalized to protein concentration, which was determined with the bicinchoninic acid (BCA) protein assay kit (Thermo Fisher Scientific, MA, USA).

In Vitro Lipid Peroxidation Inhibition Assay

Docosahexaenoic acid (DHA) was oxidized in a linoleic acid model system to measure antioxidant activity, following the method by Osawa and Namiki[76] with minor modifications. Briefly, K-115 was dissolved in PBS and added into a mixture of 5 mM DHA and an oxidizing agent (5 mM $FeSO_4$/10 mM ascorbic acid). In a parallel experiment, the sample was replaced with a standard antioxidant, BHT, as a positive control. The mixed solution was induced at 37°C for 2 hours. The oxidized DHA solution (200 μL) was added to 500 μL of a reaction mixture (0.81% SDS, 0.36% TBA, and 9% acetic acid) on ice. After heating the reaction mixture to 100°C for 1 hour, it was centrifuged at 20,000*g* for 10 minutes at 4°C. The supernatant was collected and its fluorescence was measured at 530 nm excitation and 550 nm emission.

In Situ Detection of ROS Production

FG-labeled mice were injected intravitreally with 1 μL 50 μM CellROX Green Reagent (Life Technologies, Inc.). A Hamilton syringe with a 32-gauge needle was used. Two hours after injection, the mice were perfused with ice-cold saline, followed by 4% paraformaldehyde (PFA). The eyes of the mice

Investigative Ophthalmology & Visual Science

were collected and fixed in 4% PFA for 1 hour on ice. Following fixation, the eyes were cryopreserved with increasing concentrations of sucrose and frozen in Tissue-Tek OCT compound (Sakura Finetechnical, Tokyo, Japan). For nuclear staining, 14-μm-thick cryosections were incubated in propidium iodide (PI) solution for 10 minutes. FG- and CellROX-positive cells in the GCL were counted in complete retinal sections taken through the optic nerve. To avoid fluorescence bleed-through caused by FG, fluorescence microscopy was carried out without Vectashield mounting medium.

Measurement of ROS Levels in the Retina

Two hours after the intravitreal injection of 1 μL 50 μM CellROX Green Reagent, the retinas were dissected in ice-cold Dulbecco's phosphate-buffered saline (DPBS) and frozen in liquid nitrogen. The retinas were then homogenized in radioimmunoprecipitation assay (RIPA) buffer (25 mM Tris-HCl pH 7.6, 150 mM NaCl, 1% NP-40, 1% sodium deoxycholate, 0.1% SDS) containing 1% protease inhibitor cocktail on ice, and centrifuged at 15,000*g* for 10 minutes at 4°C. The supernatant was collected and its fluorescence was measured at 485 nm excitation and 538 nm emission. The results were normalized to protein concentration, which was determined with BCA protein assay kit.

Statistical Analysis

We used an unpaired *t*-test to evaluate statistical differences in the two samples. An ANOVA followed by Dunnett's test was used to compare the mean in the three groups. Data are presented as means ± standard deviation. The level of statistical significance was set at $P < 0.05$.

Results

K-115 Exerts a Neuroprotective Effect on RGCs After NC

There are several ROCK inhibitors that have been reported to attenuate neuronal cell death after optic nerve injury.[49,59,77–79] We used a mouse NC model to determine whether K-115, a novel ROCK inhibitor, exhibited the same neuroprotective effect on RGCs. The density of RGCs in the control and PBS treatment groups was 3815 ± 430 RGCs/mm^2 and 1730 ± 196 RGCs/mm^2, respectively. Seven days after NC, the density of surviving RGCs in the K-115 and fasudil treatment groups decreased to 3022 ± 306 RGCs/mm^2 and 2846 ± 89 RGCs/mm^2, respectively (Figs. 1B–J). We also performed qRT-PCR to evaluate the neuroprotective effects of K-115 and fasudil on RGCs. This revealed that after NC, the mRNA level of *Thy-1.2*, an early marker of RGC stress, fell by approximately 70, 50, and 40% in the PBS, K-115, and fasudil treatment groups, respectively (Fig. 1K). Similarly, the mRNA level of *Brn3a*, another marker of RGC, fell by approximately 90, 80, and 70%, respectively. Our results thus demonstrated a significantly increased RGC survival rate in the K-115- and fasudil-treated group, compared to the PBS-treated group. The neuroprotective effect of K-115 was transient, as it did not promote significant RGC protection at 14 or 28 days after NC (Supplementary Fig. S1).

Inhibitory Effects of K-115 on Axonal Injury-Induced Lipid Peroxidation In Vivo

We previously found that 4-hydroxynonenal (4-HNE)- and 8-hydroxy-2′-deoxyguanosine (8-OHdG)-immunostained cells increased in the GCL after NC.[72] However, these markers do not always reflect the overall oxidative status of the retina. Therefore, we measured the total level of oxidized lipids with a TBARS assay. We found that the level of TBARS in the retina increased with time after NC. As shown in Figure 2A, 4 and 7 days after NC, oxidized lipids had increased significantly in comparison with the non-NC group (2.0 ± 0.6 vs. 3.4 ± 1.1 and 4.8 ± 0.7 nmol/mg protein). We next investigated whether K-115 inhibits lipid peroxidation in the retina after NC. We found that administration of 1 mg/kg/d of K-115, which qRT-PCR analysis of RGC markers such as *Thy-1.2* and *Brn3a* revealed was an effective concentration (data not shown), significantly attenuated the oxidation of lipids in the retina after NC (Fig. 2B). This result suggests that K-115 can inhibit the oxidative stress induced by axonal injury.

Antioxidant Effects of K-115 on the Free Radical-Mediated Oxidative System

To further determine the inhibitory effect of K-115 on lipid peroxidation after NC, we measured the TBARS level induced by free radical-mediated oxidative stress. Since it is well known that DHA is the major polyunsaturated fatty acid (PUFA) in the retina,[80] we assessed the oxidative level of DHA in an in vitro system. Our in vivo system clearly indicated that K-115 had an inhibitory effect on NC-induced lipid peroxidation. However, as the functional mechanism behind this effect remained unclear, we tried to determine if K-115 functions directly as an antioxidant. Butylated hydroxytoluene, a well-known synthetic antioxidant, efficiently delayed lipid peroxidation in comparison to an untreated group, whereas the delay in peroxidation after the administration of K-115 was significantly lower (Fig. 3). This indicated that K-115 did not, in fact, act as an antioxidant reagent in this system.

Identification of ROS-Generating Cells in the GCL After NC

Previously, our group found oxidative stress markers such as 8-OHdG and 4-HNE in the GCL after NC,[72] clearly indicating that NC induces oxidative stress. Since ROS, including free radicals such as superoxide anions and hydroxyl radicals, are one of the main contributors to oxidative stress, we attempted to identify the major source of ROS production in the GCL by performing double labeling with the retrograde tracers FG and CellROX, since these accumulate in the mitochondria and nucleus. As shown in Figure 4A, the cells in the GCL that were positive for the CellROX fluorescence signal were mostly RGCs. Interestingly, however, some cells in the inner nuclear layer (INL) also produced ROS 4 days after NC. The percentages of FG/CellROX double-positive cells among the GCL cells 1, 4, and 7 days after NC were 58, 88, and 73%, respectively (Fig. 4B). The percentage of non-RGC cells positive for CellROX cells in the GCL reached a maximum of 11% on day 4. These results indicate that production of ROS after NC occurs mainly in RGCs.

K-115 Suppressed the Time-Dependent Production of ROS in RGCs After NC Injury

As shown in Figures 4A and 4B, CellROX labeling identified the location of ROS production, indicating that oxidative stress is mainly induced in RGCs after NC. Furthermore, as shown in Figure 1, K-115 dramatically altered the RGC death rate after NC. This prompted an investigation of K-115's role in suppressing ROS production in RGCs using an in vivo model, by first inducing ROS production with NC, and then assessing the level of CellROX fluorescence. We found that after NC, the percentage of FG/CellROX double-positive cells gradually

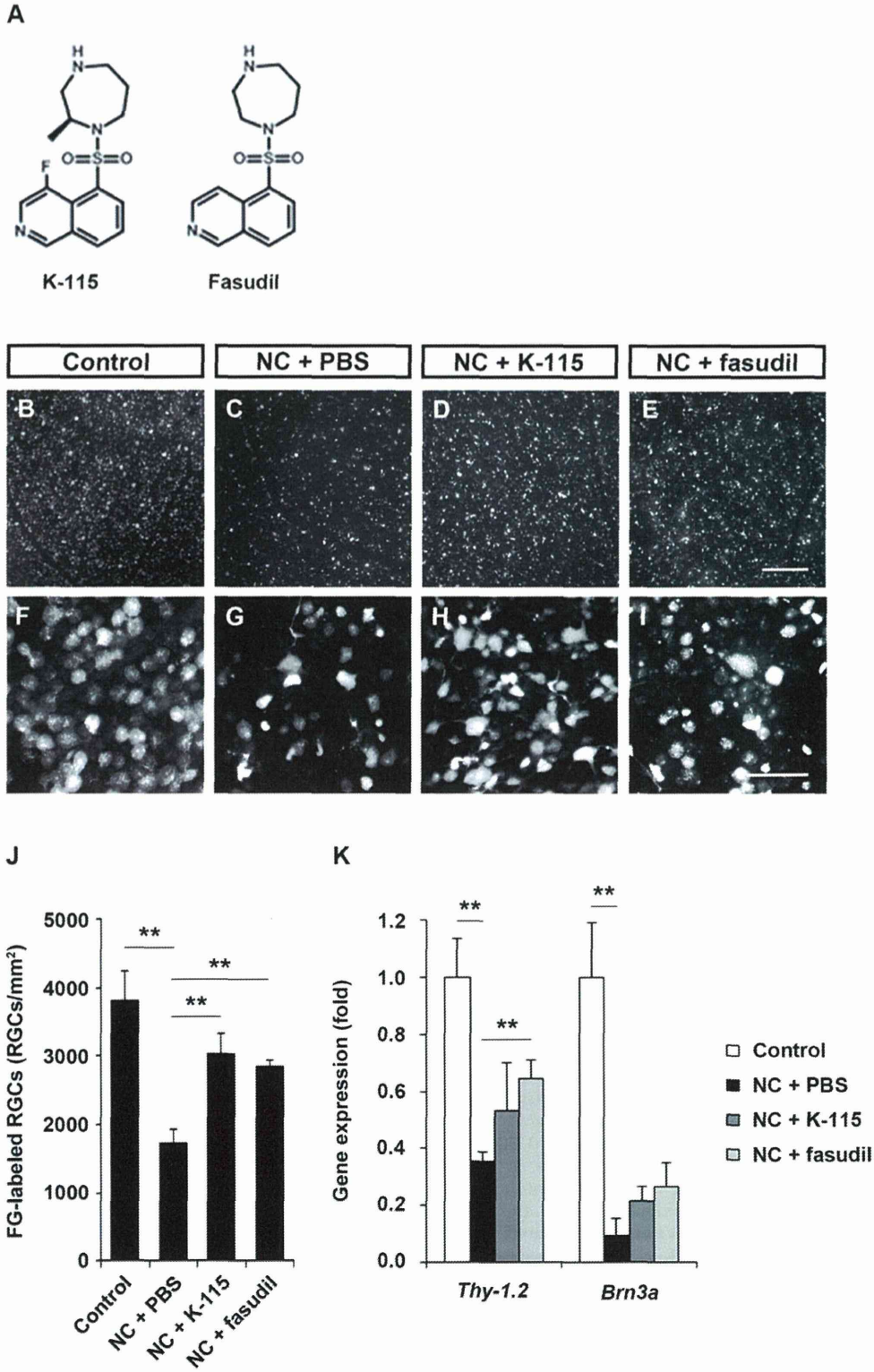

FIGURE 1. K-115 and fasudil exerted a neuroprotective effect on RGCs after NC. (**A**) Chemical structures of K-115 and fasudil. (**B–I**) Representative images of retrogradely labeled RGCs. (**B–E**) Higher-magnification versions of the upper panels. *Scale bars*: 200 μm (**B–E**) 50 μm (**F–I**). (**J**) Oral administration of K-115 or fasudil (1 mg/kg daily) for 7 days significantly delayed cell death in post-NC RGCs ($n = 6$ in each group). (**K**) Treatment with K-115 or fasudil also delayed a reduction in mRNA of *Thy-1.2* and *Brn3a*, RGC markers. Glyceraldehyde-3-phosphate dehydrogenase (*GAPDH*) was used as an internal standard (**$P < 0.01$; *error bars*, SD; $n = 4$ in each group).

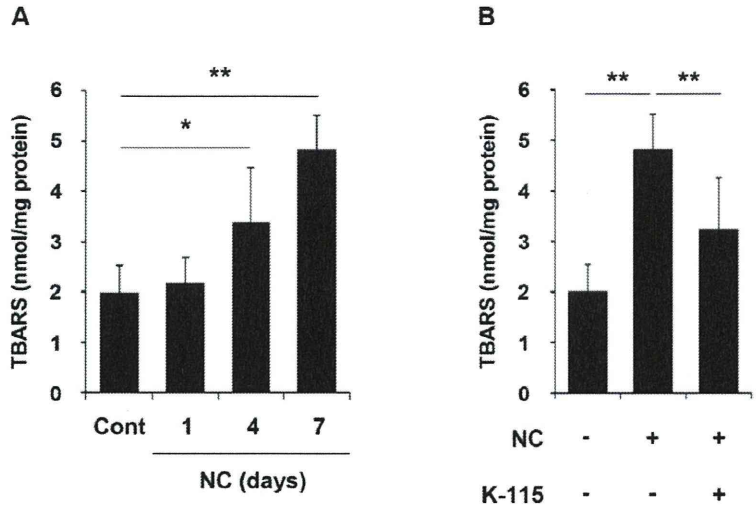

FIGURE 2. Inhibitory effects of K-115 on axonal injury-induced lipid peroxidation in vivo. (**A**) After NC, the level of lipid peroxidation increased in a time-dependent manner in the retina compared with the nontreated control group ("Cont"). (**B**) Daily administration of K-115 for 7 days significantly inhibited lipid peroxidation in mice after NC (*$P < 0.05$, **$P < 0.01$; *error bars*, SD; $n = 6$ in each group).

increased, reaching a maximum of 94% on day 4 before decreasing to 78% on day 7 (Figs. 5A, 5B). With K-115 treatment, although the percentage of CellROX-positive RGCs decreased in a time-dependent manner for 7 days, at all time points the percentage of double-positive cells was at least 40% lower than with PBS treatment. We also found that CellROX fluorescence intensity in the retinal lysate was significantly increased after NC, and that this elevated intensity was almost completely suppressed by administration of K-115 (Fig. 5C). These results indicate that K-115 treatment, rather that inhibiting downstream ROS production after NC, such as lipid peroxidation, inhibits ROS production itself through an indirect mechanism.

Involvement of the Nox Family in NC-Induced ROS Production

As previous reports indicated that the Rho/ROCK pathway is involved in inducing the Nox family,[22,81,82] we also performed an investigation of the involvement of this family with ROS production after NC. After NC, the mRNA levels of *Nox1*, *Nox2*, and *Nox4* in the PBS treatment group increased 5.6-, 3.2-, and 5.7-fold relative to the control group (Fig. 6A). While K-115 had an inhibitory effect on NC-induced up-regulation of *Nox1*, it had no effect on *Nox2* and *Nox4*. We next considered the direct involvement of the Nox family in NC-induced ROS production. We found that within 5 minutes of treatment with the Nox inhibitor VAS2870 after NC, CellROX fluorescence was almost completely eliminated. This suggests that almost all ROS production is derived from *Nox1*.

Discussion

The results of the present study strongly suggest that K-115, a ROCK inhibitor, can prolong RGC cell survival by suppressing oxidative stress through pathways involving the Nox family (Fig. 7).

Both our present study and previous studies by others have shown that oxidative stress is involved in RGC death after axonal injury.[17,72,83–89] In order to evaluate the efficacy of K-115, we compared the density of FG-labeled RGCs in mice treated with either PBS or ROCK inhibitors such as K-115 and fasudil 7 days after NC, in addition to the qRT-PCR analysis of RGC markers. We found that the neuroprotective effects of K-115 and fasudil after NC were similar, but that the specificity of the effect of K-115 on ROCK was 2 to 18 times higher than that of fasudil. This might have been related to our finding that the concentration-dependent neuroprotective effect of K-115 and fasudil against active ROCK in the retina after NC reached a plateau at 1 mg/kg/d. We therefore speculate that both ROCK inhibitors have a similar protective effect against axonal injury. Additionally, we found that K-115 dramatically suppressed oxidative stress, including ROS production by the RGCs themselves. Although the precise mechanism by which K-115 suppresses ROS production after NC has not yet been adequately determined, our present results strongly indicate that K-115 does not directly function as an antioxidant (Fig. 3). Moreover, we confirmed that expression of *Nox1*, which is strongly related to ROS production after NC, decreased with K-115 treatment. Based on previous findings that fasudil, a compound whose structure is similar to K-115, had an indirect antioxidant effect in various disease models including hyper-

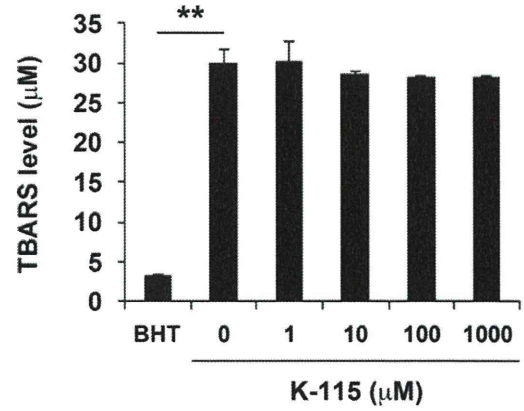

FIGURE 3. Antioxidative effects of K-115 on the free radical-mediated oxidative system. The synthetic antioxidant BHT (50 mM) delayed lipid peroxidation efficiently, but K-115 (1–1000 μM) did not show an antioxidative effect (**$P < 0.01$; *error bars*, SD; $n = 3$ in each group).

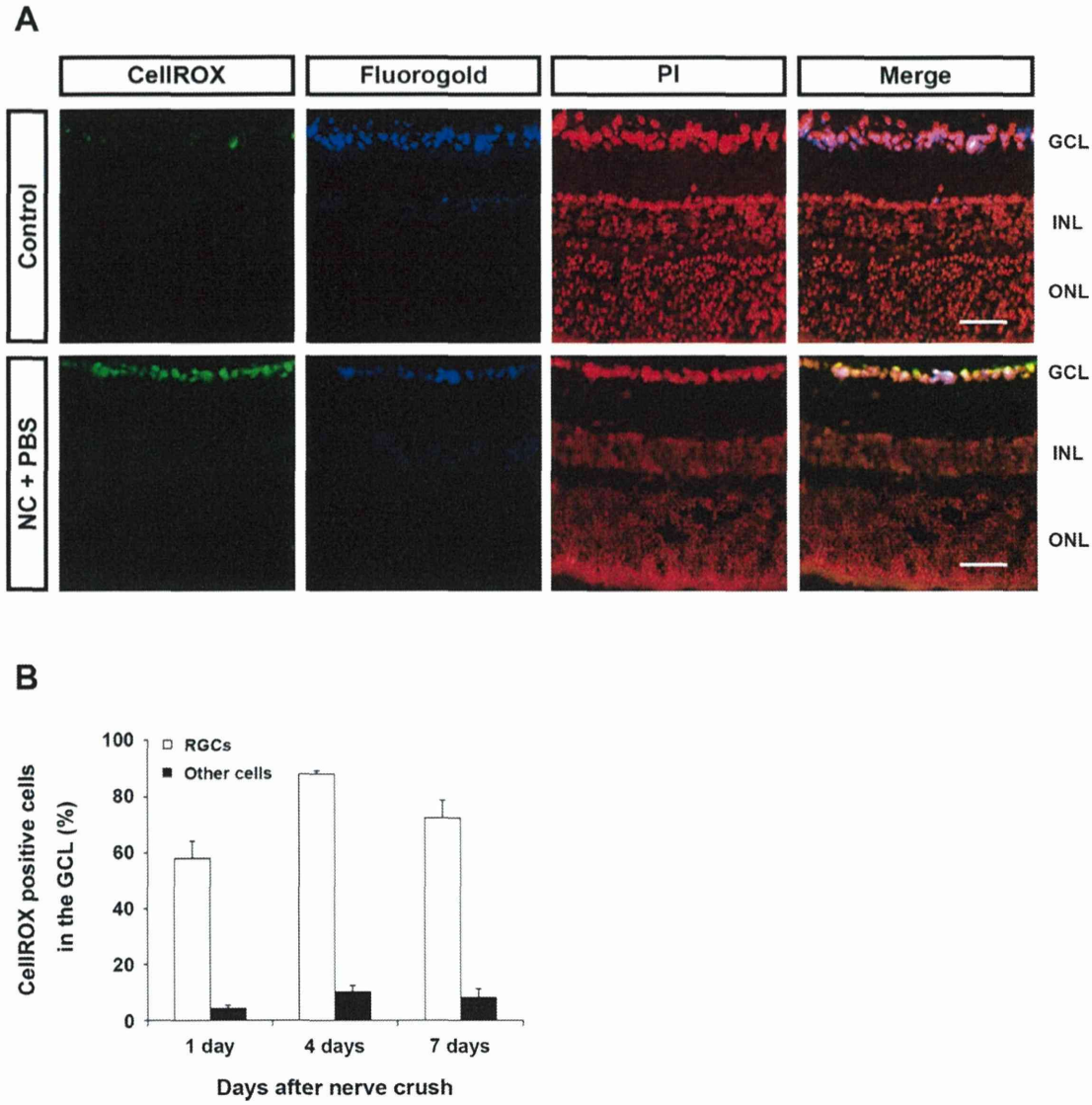

FIGURE 4. Identification of ROS-generating cells in the GCL after NC injury. (**A**) Representative fluorescence images of frozen sections showing ROS-producing cells (shown in *green*) in the GCL on day 4 after NC. *Scale bars*: 50 μm. (**B**) Quantification of the number of FG-positive (shown in *blue*) or -negative cells among the CellROX-labeled cells on days 1, 4, and 7 after NC injury (day 1 $n = 4$, days 4 and 7 $n = 6$). Cell counting results are shown as the ratio of FG- and CellROX-positive cells (i.e., RGCs) or FG-negative and CellROX-positive cells (i.e., other cells) to the number of PI-positive cells (*red*) in each section.

cholesterolemia,[90] diabetes,[91] and ischemia,[92] it is possible that K-115 also had a similar antioxidant effect in our NC model.

Oxidative stress is implicated in neuronal cell death in many neurodegenerative diseases, such as Alzheimer's disease,[34] amyotrophic lateral sclerosis,[93] and Parkinson's disease.[94,95] In glaucoma it has been reported that increases in oxidative stress markers can be found in a patient's aqueous humor and plasma.[86,87] Our research to date, using an experimental glaucoma model, strongly suggests that glaucoma should also be considered as a chronic neurodegenerative disease associated with oxidative stress. One widely accepted measurement of oxidative stress is the TBARS assay. Lipid peroxides, unstable indicators of oxidative stress in cells, decompose to form more complex and reactive compounds. Measurements of these end products indicate the level of oxidative damage. Our study demonstrated that the TBARS level in the entire retina increased with time after NC, and was highest on the seventh day. However, as indicated in our previous report, oxidative stress appears to be higher in RGCs than in any other layer of the retina.[72] Therefore, we suggest that oxidative stress-induced RGC death directly affects the survival of RGCs after NC. To protect RGCs from oxidative stress, we examined the effects of the ROCK inhibitor K-115, and found that it could inhibit increases in the TBARS level. In other words, K-115 can suppress oxidative stress after NC.

ROCK inhibitors have been widely used as treatments for various neurological disorders, including spinal cord injuries,[32,35–38] stroke,[39–46] multiple sclerosis,[32] and Alzheimer's disease.[32–34] It has previously been reported that targeting small Rho GTPase has a positive dose-dependent effect on the regeneration of RGCs after injuries such as NC.[49,59,77–79] In the axonal injury model, it has been reported that ROCK activity